

Supplementary Information for

Label-free and live cell imaging by interferometric scattering microscopy

Jin-Sung Park^a, Il-Buem Lee^{a,b}, Hyeon-Min Moon^{a,b}, Jong-Hyeon Joo^{a,c}, Kyoung-Hoon Kim^{a,b},
Seok-Cheol Hong^{a,b} & Minhaeng Cho^{a,c}

^aCenter for Molecular Spectroscopy and Dynamics, Institute for Basic Science, Seoul 02841, Korea,

^bDepartment of Physics, Korea University, Seoul 02841, Korea,

^cDepartment of Chemistry, Korea University, Seoul 02841, Korea.

AUTHOR INFORMATION

*Corresponding Authors

mcho@korea.ac.kr or hongsc@korea.ac.kr

J.-S. P. and I.-B. L. contributed to this work equally.

Contents

Figure S1. Schematic of the light path reflected from the cube-type beamsplitter.

Figure S2. The measurement of beam size illuminated to the image focal plane.

Figure S3. Background subtraction in iSCAT images.

Figure S4. Analysis of a standing angle of *E. coli* OP50 thermally fluctuating on a glass substrate.

Figure S5 Two different types of fringe patterns observed in cytoplasm.

Figure S6. iSCAT live-cell imaging of budding yeast *Saccharomyces cerevisiae*.

Figure S7. Zoomed-in image for Fig. 5.

Figure S8. Another example of the phase contrast and iSCAT cell images for the same fixed COS-7 cells .

Video-E coli.avi

Video-yeast.avi

Figure S1

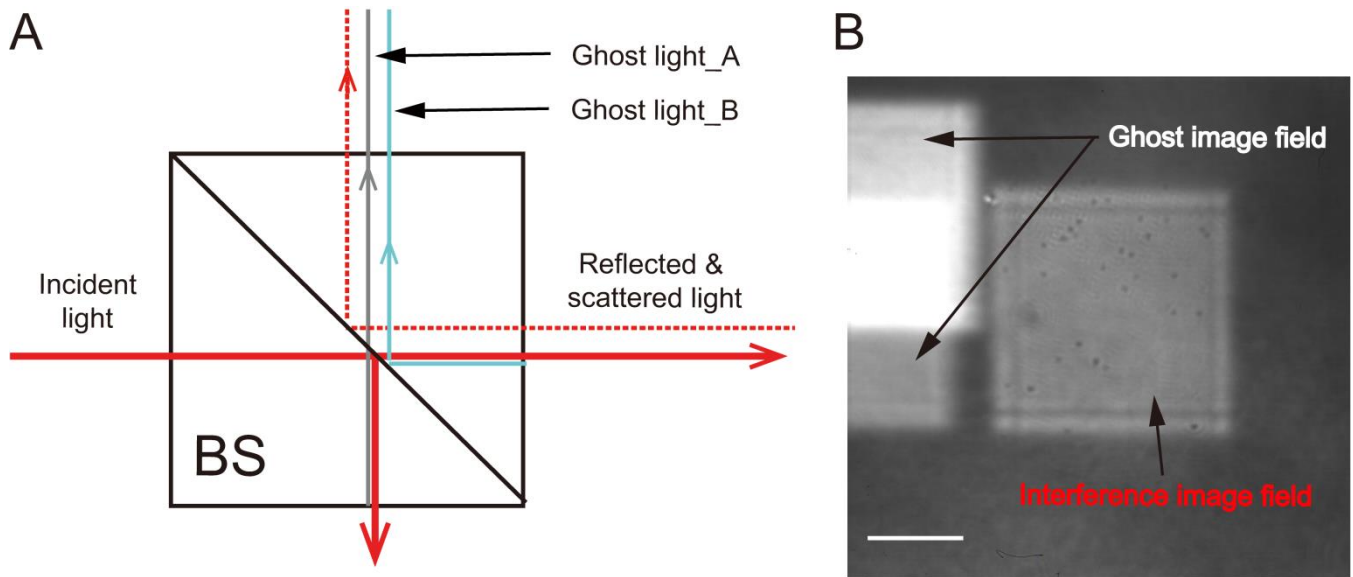


Fig. S1 Schematic diagram of the beam paths effected by reflections from various surfaces of the cube-type beamsplitter (BS) (A) and two ghost fields and one real field from the target area shown in the full field of view ($23 \times 23 \mu\text{m}^2$) of a CMOS camera (B). Here, the viewfield of real iSCAT image is $10 \times 10 \mu\text{m}^2$, and the scale bar in (B) is $4 \mu\text{m}$.

Figure S2

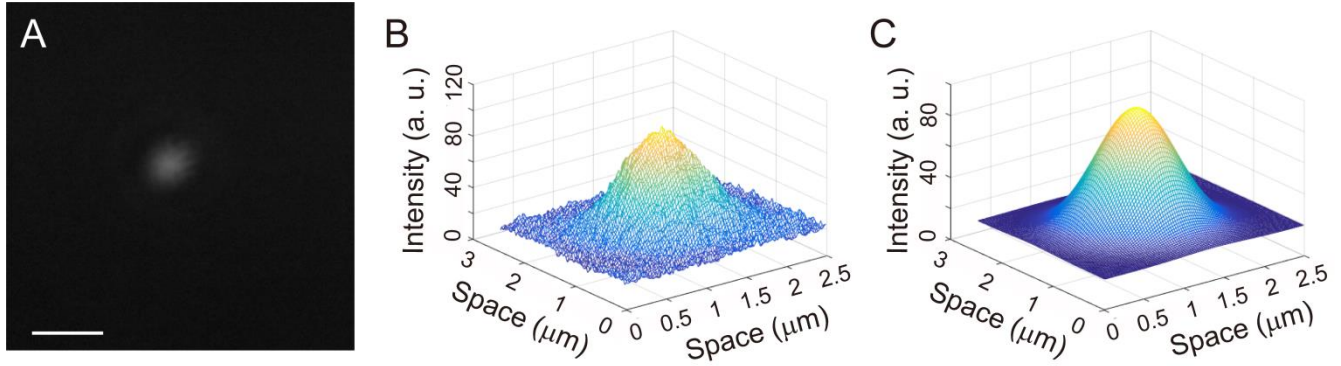


Fig. S2 Measurement of size of the beam illuminated on the image focal plane. (A) A raw image of illuminated beam. (B) A 3-dimensional intensity plot obtained from (A). (C) Elliptical Gaussian fit from (B). To calculate a beam diameter, we used the elliptical Gaussian function,

$$f(x, y) = A \exp\left(-\left(\frac{(x - x_0)^2}{2\sigma_x^2} + \frac{(y - y_0)^2}{2\sigma_y^2}\right)\right)$$

where the coefficient A is the amplitude, x_0 and y_0 are the coordinates of a beam center, and σ_x and σ_y are the ‘size’ of a beam spot. From this equation, we defined the beam diameter as the full width at half maximum (FWHM), $\text{FWHM} = 2\sqrt{2\ln 2}\sigma \cong 2.35\sigma$. Here, we used $\langle \bar{\sigma} \rangle = (\sigma_x + \sigma_y)/2$. According to our fit, the focused beam has a diameter of ~ 900 nm. The scale bar in (A) is $2 \mu\text{m}$.

Figure S3

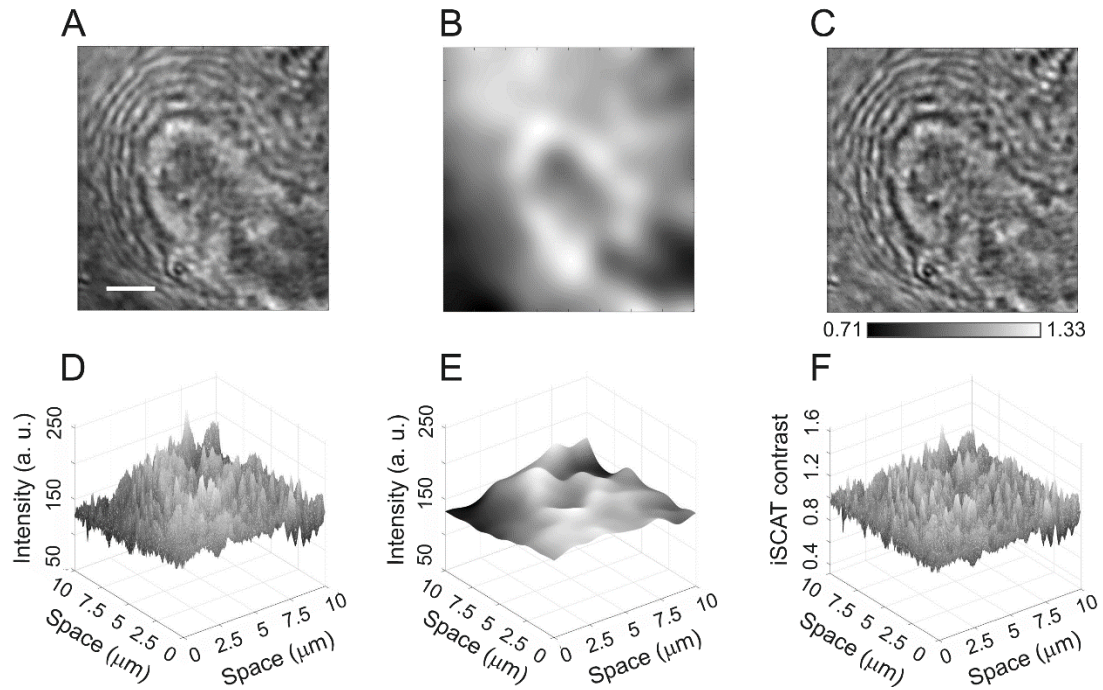


Fig. S3 Background subtraction in iSCAT images. (A) Original iSCAT snapshot of a cell nucleus and its neighboring area. (B) Background image calculated by 10×10 binning from (A). (C) Processed image through background subtraction. (D, E) 2D intensity profiles of iSCAT image corresponding to (A) and (B). (F). 2-D contrast profile of the processed iSCAT image in (C). The scale bar in (A) is $2 \mu\text{m}$.

Figure S4

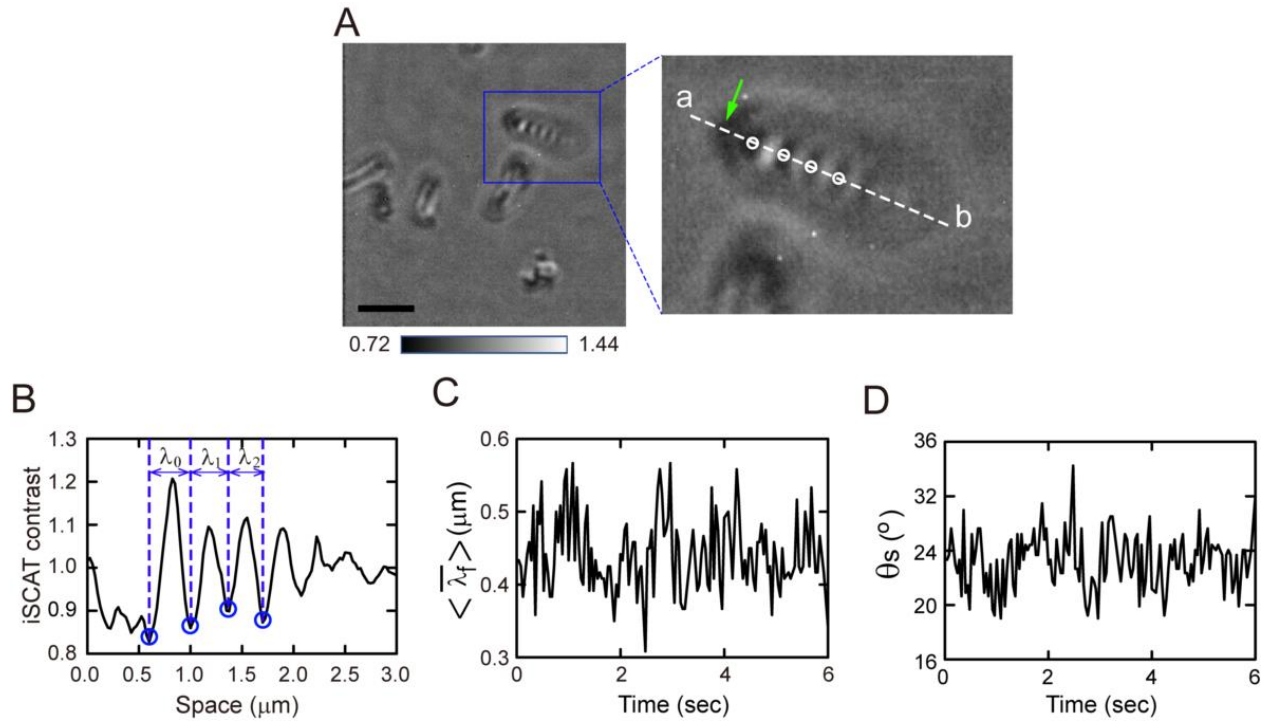


Fig. S4 Analysis of a standing angle of *E. coli* OP50 thermally fluctuating on a glass substrate. (A) Snapshot image of bacteria *E. coli* OP50 with a periodic fringe pattern alternating in intensity (see Supplementary video-E Coli.avi). Here, the head of bacteria, which is indicated by the arrow in the magnified view of the blue boxed area in (A), is anchored on a substrate with a slight tilt angle. (A) The space plot showing the fringes taken along the line drawn through the center of the bacteria (dotted line in the magnified view of (A)). The blue circles in the graph (B) indicate the positions of intensity minima in the fringe formed along the body of the bacteria in (A). (C, D) The changes of periodicity in the fringe pattern (C) and its corresponding variation in the standing angle (θ_s) of bacteria (D) (see Supplementary video-E coli.avi). Here, the wavelength of the fringe is obtained as $\langle \bar{\lambda}_f \rangle = (\lambda_0 + \lambda_1 + \lambda_2)/3$ by averaging the first three fringe intervals from the first to fourth peaks and the variation in a standing angle is calculated by $\theta_s = \arctan(\lambda_i / (2 \times n \times \langle \bar{\lambda}_f \rangle))$. Here, λ_i and n are the wavelength of incident light (405 nm) and the refractive index of a culture medium ($n = 1.3$), respectively.

Figure S5

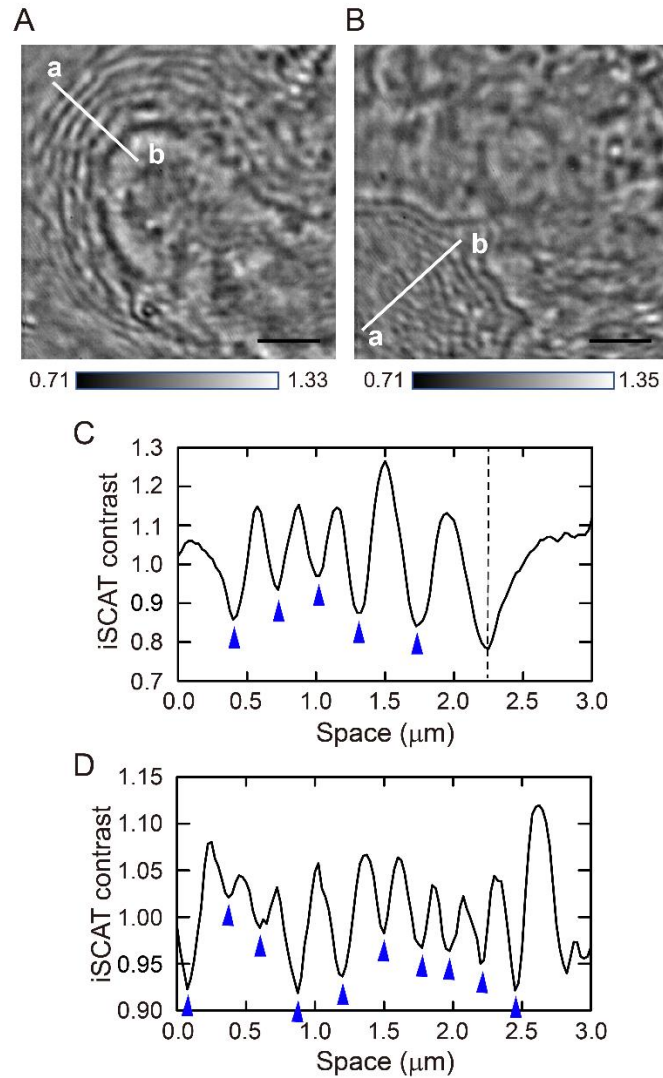


Fig. S5 Two different types of fringe patterns observed in cytoplasm. (A) The labyrinth-like fringe pattern with a wavelength of sub-micrometer ($\langle \bar{\lambda}_f \rangle = 0.43 \pm 0.09 \mu\text{m}$, for $N = 4$) surrounds the organelle with an oval shape shown in the blue dashed-line box of Fig. 3. (B) The irregular fringe pattern exhibits shorter wavelength ($\langle \bar{\lambda}_f \rangle = 0.34 \pm 0.05 \mu\text{m}$, for $N = 9$) that the labyrinth fringes in (A). (C, D) The iSCAT contrast variations along the dashed lines from 'a' to 'b' in (A) and (B) are plotted. The boundary between the organelle membrane and cytosol is marked by a vertical dotted line in (C). The scale bars in (A) and (B) are $2 \mu\text{m}$.

Figure S6

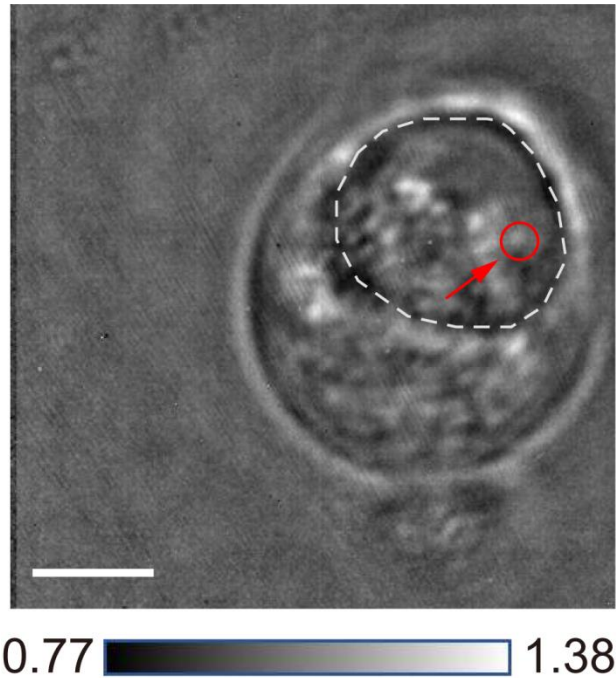


Fig. S6 iSCAT live-cell imaging of budding yeast *Saccharomyces cerevisiae*. The dotted line indicates the outer boundary of a vacuole which acts as a variety of secretory, excretory, and storage functions within a yeast cell. Also, the active motion of an amorphous mass (here we call a dancing body) is visible and can be tracked in a time lapse mode (see Supplementary video-yeast.avi).

Figure S7

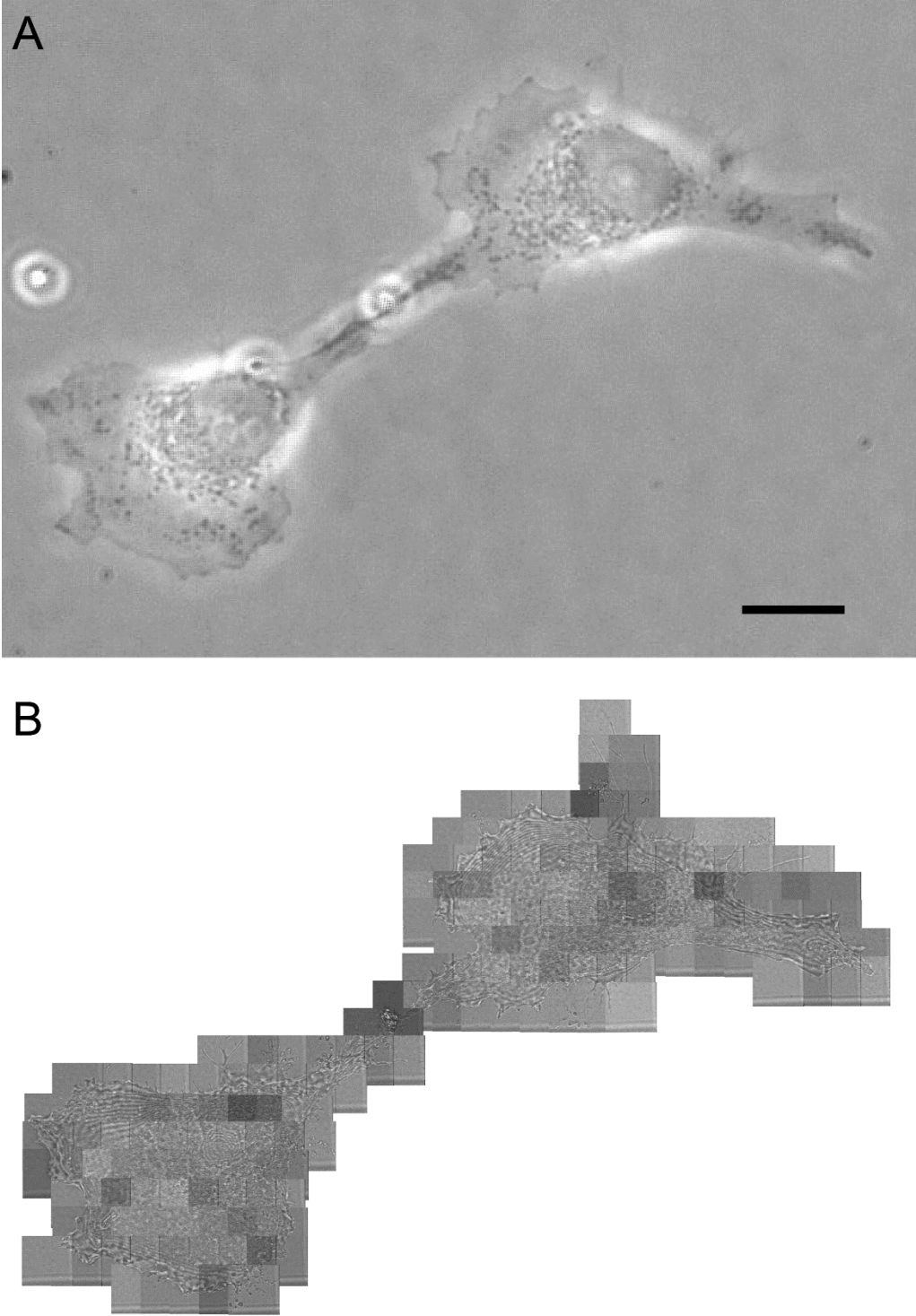


Fig. S7 Zoomed-in images of fixed COS-7 cells taken by the phase contrast and iSCAT microscopy, which are presented in Fig. 5. The scale bar in (A) is 20 μm

Figure S8

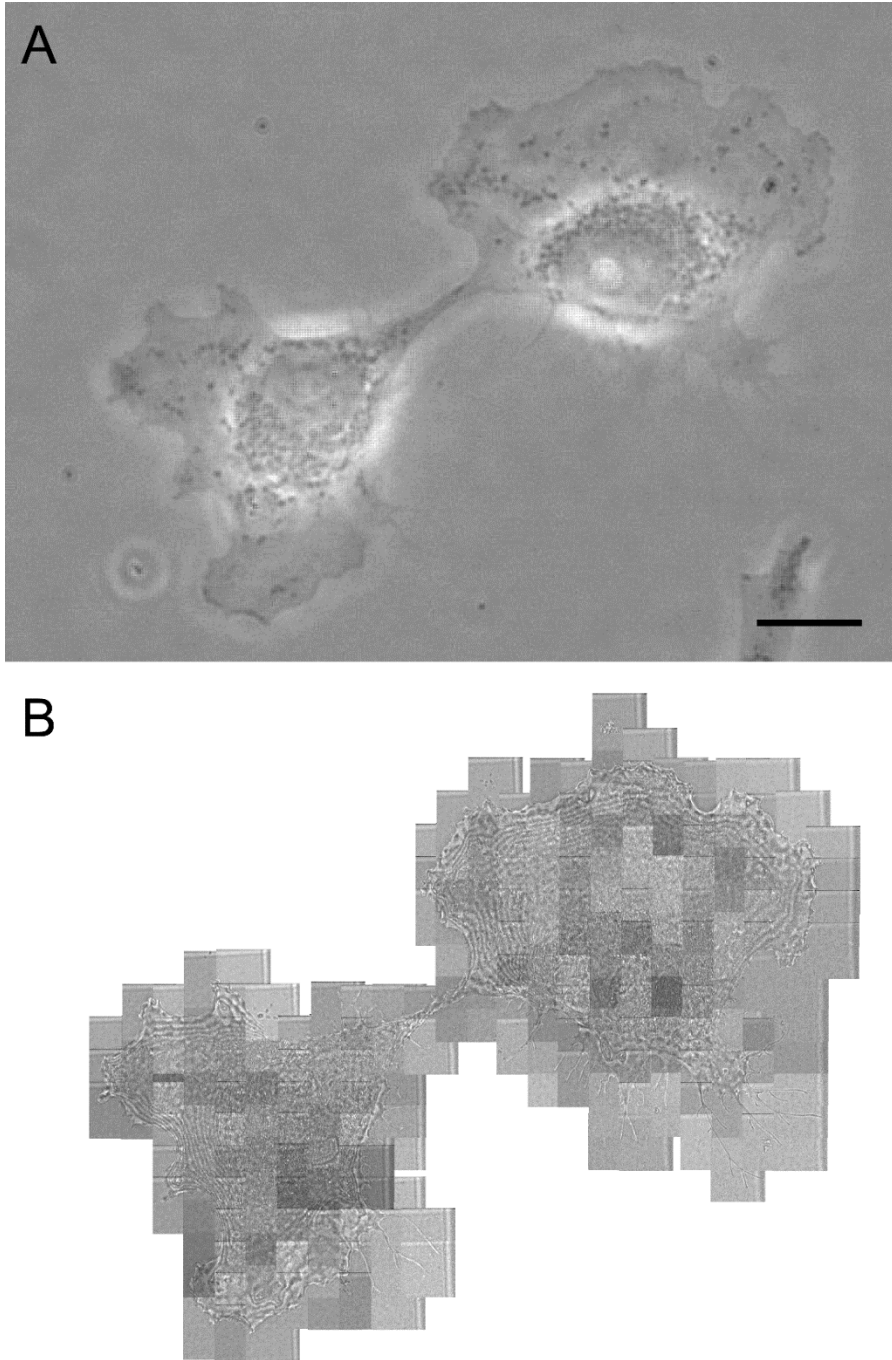


Fig. S8 Another example of the phase contrast (A) and iSCAT image (B) taken for the same fixed COS-7 cells. Here, the iSCAT image (B) is constructed with a total 225 iSCAT snapshots. The scale bar in (A) is 20 μm .